Biochimica et Biophysica Acta, 1145 (1993) 141–148

BBAMEM 75832

Configurational entropy is the driving force of ethanol action on membrane architecture

Da-Cheng Wang, Theodore F. Taraschi, Emanuel Rubin and Nathan Janes

Department of Pathology and Cell Biology, Medical College of Thomas Jefferson University, Philadelphia, PA (USA)

(Received 23 June 1992)

Key words: Ethanol; Partition; Configurational entropy; Phase equilibrium; Anesthetic; EPR

A colligative thermodynamic framework is developed to describe the action of ethanol on membranes. The partitioning of ethanol into a membrane structure imparts a randomness, configurational entropy, that stabilizes that structure from an energetic standpoint. When partitioning between membrane structures differs, the equilibrium between them is altered to favor the structure with the largest partition coefficient for ethanol. The action of ethanol and temperature originate in entropy and are equated through entropy. Membrane equilibria that are predicted to be most sensitive to the action of ethanol (where dilute concentrations of ethanol cause a perturbation equal to a large change in temperature) are those that exhibit a small thermal entropy change and a large difference in solute partitioning between membrane structures. Our model predicts that ethanol does not act on a single membrane structure, but on both structures in an equilibrium. The thermodynamic framework is applied to the action of ethanol on cooperative equilibria in a dipalmitoyl lecithin model membrane. Ethanol-induced perturbations are monitored by electron paramagnetic resonance (EPR) using the spin label, Tempo. The equilibrium between the gel and ripple-structures ($L_{\beta'} \rightarrow P_{\beta'}$, pretransition) exhibits a small change in thermal entropy and, as predicted, is more sensitive to the action of ethanol than the equilibrium between the ripple and fluid bilayer-structures ($P_{\beta'} \rightarrow L_{\alpha}$, main transition) which exhibits a large thermal entropy change. The framework suggests that ethanol acts through entropy, as does temperature, thereby upsetting the natural thermal balance that maintains membrane architecture.

Introduction

Many pharmacological [1] and pathological effects [2] of ethanol are postulated to originate in membrane perturbation. By the turn of the century, Hans Meyer [3] had classified ethanol as a prototypic member of a group of anesthetics that he termed the 'alcohol narcotics', which included most organic solvents. Independently, Meyer and Overton [4] noted that the anesthetic potency of these agents correlated with their olive oil/water partitioning and concluded that anesthetics act upon the lipoids of the cell. Subsequently, many lipid based theories for acute alcohol and anesthetic action have been propounded (reviewed in Ref. 5). Hill and Bangham [6] first proposed a homeostatic mechanism whereby the organism adapts to chronic ethanol exposure by remodeling the membrane structure. This adaptive response to long-term ethanol consumption was confirmed by the demonstration that a variety of membranes obtained from ethanol-fed animals were resistant to ethanol-induced decreases in membrane order reported by spin-labels [7] and resistant to the partitioning of a variety of lipophilic agents, including ethanol [8]. Chronic ethanol consumption is associated with disease in a variety of tissues. A parsimonious interpretation rejects a unique organ-specific pathogenesis in favor of a unitary approach based on the commonalty of chronic membrane perturbation [9].

While lipid theories of acute ethanol and anesthetic action are generally acknowledged to qualitatively reproduce the anesthetic potencies observed in the organism, lipid theories are criticized on quantitative grounds due to membrane insensitivity to concentrations of alcohols and anesthetics consistent with consciousness [10]. These quantitative arguments have led some to propose that anesthetic action is mediated directly through specific protein binding [10,11]. A major impetus to the protein theories was the surprising observation that anesthetics of a wide range of size, charge, and polarity inhibited a purified, lipid-free protein (luciferase) to a degree that paralleled five

Correspondence to: N. Janes, Department of Pathology and Cell Biology, Medical College of Thomas Jefferson University, 1020 Locust Street, Philadelphia, PA 19107, USA.

Abbreviations: DPPC, 1,2-dipalmitoyl-*sn*-glycero-3-phosphocholine; EPR, electron paramagnetic resonance; Tempo, 2,2,6,6-tetramethylpiperdine-1-oxyl.

orders of magnitude of an agent's oil solubility [11]. In the traditional lock and key model for protein-ligand binding, the idea that a 'lock' could accommodate such diverse 'keys' was quite unexpected. Recently, however, the luciferase model for anesthesia was shown not to reproduce the antagonistic relationship between pressure and alcohol/anesthetic potency [12]. Therefore, no protein model qualitatively reproduces the observed behavioral potencies of anesthetics, and no lipid model quantitatively reproduces the observed potencies. Thus, the challenge for proponents of lipid theories is to understand the origins of sensitivity to alcohol and anesthetic action.

We have reformulated the Meyer-Overton hypothesis using a generalized colligative thermodynamic framework [13–15]. This framework implicates configurational entropy as the driving force of alcohol action, equates the action of ethanol and temperature through entropy, and predicts that cooperative equilibria in membranes between structures of similar thermal entropy are especially susceptible to alcohol action. The thermodynamic predictions are tested for ethanol by monitoring the ability of ethanol to perturb two cooperative (phase) equilibria in lecithin membranes. The equilibrium between the gel and ripple structures involves structures of similar thermal entropy, whereas the equilibrium between the ripple and fluid bilayer structures involves, by comparison, structures of greatly different thermal entropies [16]. Ethanol action is interpreted from the standpoint of competing contributions of entropy – the configurational entropy imparted to the membrane by ethanol versus the thermal entropy change characteristic of the structural interchange.

Materials and Methods

Analysis of Tempo partitioning

Tempo (2,2,6,6-tetramethylpiperdine-1-oxyl) partitioning is obtained using deconvolution by spectral difference and double integration as described in Results and shown in Fig. 1.

The Tempo partition coefficients obtained are considered characteristic of a lipid state and fit to the following expression.

$$K_p = \frac{K_p^{\alpha} + K_p^{\beta} \exp C(T - T_m)}{1 + \exp C(T - T_m)} \tag{1}$$

$$K_p^i = m_i T + b_i \tag{2}$$

$$C = \frac{\Delta H_{vH}}{RTT_m} \simeq \frac{\Delta H_{vH}}{RT_m^2} \tag{3}$$

The partition coefficient for the membrane states α and β are K_p^{α} and K_p^{β}, respectively, and include a temperature dependence that is fit linearly. Partition coefficients are expressed in molal units, (mol Tempo/kg lipid)/(mol Tempo/kg buffer). The total partition coefficient is K_p and the midpoint temperature is T_m. A fit of the experimental data to this function yields temperature-dependent partition coefficients for each phase, midpoint temperatures, and van't Hoff enthalpies. The van't Hoff enthalpy (ΔH_{vH}) of phospholipid dispersions is a measure of the sharpness of the transition, and is larger than the actual calorimetric enthalpy (ΔH_{cal}), because cooperativity is finite in these systems [17].

Analysis of ethanol action

In thermodynamic terms, the partitioning of solutes into a membrane structure increases the positional randomness of the assembly and stabilizes it. This stabilization stems from an additional entropic term, configurational entropy, that is competitive with thermal entropy in altering the free energy of a membrane assembly. On a mole fraction basis the configurational entropy, S_{cf}, of any component, n, in a mixture is deduced from probability theory [18] as follows:

$$S_{cf(i)} = -(R/N_o) \ln(n_i/\Sigma n_i) = -R \ln N_i \tag{4}$$

where R is the ideal gas constant, N_i is the mole fraction of the ith component on a molar basis, and N_o is the normalization factor. The sensitivity of membrane phase equilibria to anesthetics is dependent on the relative magnitudes of the two entropic terms.

$$\Delta T/T_m = \Delta S_{cf}/\Delta S_t \tag{5}$$

The thermal entropy change is ΔS_t. ΔT is the perturbation of the equilibrium midpoint temperature.

A simplified colligative thermodynamic framework (freezing point depression model), that made a priori assumptions about partitioning, was first applied to the main transition of phospholipids by Hill using the activity formalism, [19,20] and later extended by others [21,22]. Most recently Ueda and co-workers have examined the imperfections in Hill's treatment and recognized the importance of differences in partitioning between states in anesthetic action on the main transition and drawn conclusions that are complementary to some concepts presented here [23–25]. The generalized thermodynamic framework presented here in terms of configurational entropy makes no assumption about partitioning and is broadly applicable to all cooperative membrane equilibria.

Preparation of liposomes

Lipids (Avanti Polar Lipids, Alabaster, AL) in chloroform are dried under dry nitrogen, and evacuated (approx. 5 mTorr) for a minimum of 4 h to remove trace solvent. Multilamellar liposomes are hydrated by

vigorous vortexing in the buffer (150 mM NaCl, 10 mM Tris, 100 μM Tempo, and ethanol) at 50°C. Typical samples contain 20 mg lipid and 200 μl buffer. Lipid to probe ratios are greater than 1000.

Electron paramagnetic resonance

The EPR experiments are performed on a Bruker Instruments ER 200D EPR spectrometer. Temperature measurements are accurate to ±0.5°C. The EPR spectrometer is interfaced to an IBM system 9000 computer, which is used for data acquisition and processing. Samples are placed in a quartz flat cell and centered within the limits of the cavity for quantitative operation. Samples are equilibrated at each temperature for ten minutes, and thereafter spectra are continuously recorded until stabilized. The aqueous and lipid resonances are resolved by spectral subtraction as described in Results. The separated derivative spectra are double integrated to obtain a ratio of bound and free label. Spectral conditions: EPR operates at 9.63 GHz with 0.5 mW microwave power, 1 G modulation amplitude, 20 G sweep width, 3 or 4 scans. Representative partitioning traces are shown. Uncertainties in the midpoint temperature are ±0.5°C. The uncertainty in Tempo partitioning is dependent on the lipid/water ratio. In the traces shown (100 mg/ml), the uncertainties are as follows: $L_{\beta'}$, ±0.4; $P_{\beta'}$, ±0.6; L_{α}, ±1.5 molal units.

Results

Spectral deconvolution and double integration

The aqueous and lipid environments of Tempo exhibit slightly different isotropic hyperfine coupling constants and *g*-factors that facilitate resolution of the high-field hyperfine resonance. Previous work with Tempo generally employed the *f*-parameter [26]. The *f*-parameter is a simple ratio of bound and free peak intensities, and is not proportional to partitioning in most cases since the linewidths of the bound label vary according to the 'fluidity' of the membrane. Artifactual breakpoints in the Arrhenius plot may result [27]. We employ a spin-counting protocol to determine partitioning. The method is illustrated in Fig. 1. The overlapping bound and free resonances of Tempo in the derivative spectrum of the high-field hyperfine lines (Fig. 1A) are resolved by spectral subtraction. Spectra of aqueous solutions of Tempo obtained in the absence of lipid (Fig. 1B) are subtracted from the spectra of the lipid dispersions to yield the membrane-bound resonance alone (Fig. 1C). The resolved spectra (Figs. 1B, 1C) are double integrated to spin count the free and membrane-bound probe and calculate the partition coefficients.

A typical spectral series is excerpted in Fig. 2. The upper trace is dominated by the high field aqueous resonance. Increases in partitioning are evidenced by the growth of a low-field peak arising from membrane-bound Tempo in the lower traces.

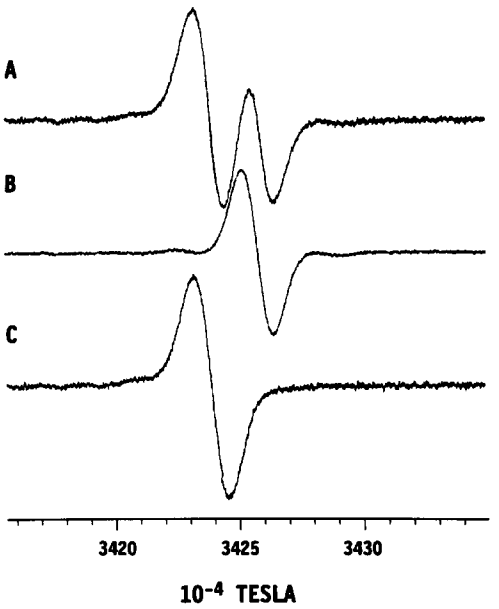

Fig. 1. Electron paramagnetic resonance first-derivative spectra of the high-field hyperfine resonance of Tempo illustrating the method of deconvolution by spectral subtraction. (A) Tempo spectrum from an aqueous dispersion of DPPC showing overlapping resonances from membrane-bound and aqueous Tempo. (B) Tempo spectrum from an aqueous buffer lacking lipid. (C) Difference spectrum (A – B) yields membrane-bound Tempo resonance.

Ethanol action on lecithin membranes

The lecithin membrane, DPPC (1,2-dipalmitoyl-*sn*-glycero-3-phosphocholine), adopts three well-studied structures or phases, a gel-structure ($L_{\beta'}$), a ripple-

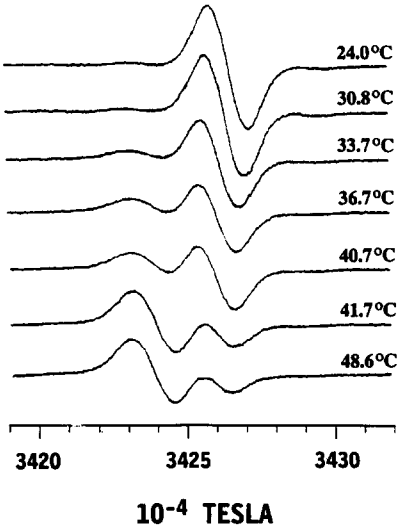

Fig. 2. The temperature dependence of selected derivative spectra of the high-field hyperfine resonance of Tempo are shown. The spectra are analyzed according to Fig. 1 and used to construct the partitioning curve shown in Fig. 3A.

structure ($P_{\beta'}$), and a fluid bilayer-structure (L_α) [16]. Since the interchange between these three membrane structures is driven by entropy, changes in solute, temperature and pressure alter the energetic balance to favor a given structure. The $L_{\beta'} \rightarrow P_{\beta'}$ equilibrium (pretransition) exhibits an equilibrium midpoint temperature determined by calorimetry as 34.8°C [16]. This change in state is accompanied by a small change in thermal entropy (12.5 $J\,mol^{-1}\,K^{-1}$). The $P_{\beta'} \rightarrow L_\alpha$ (main transition) exhibits an equilibrium midpoint temperature determined by calorimetry as 41.0°C. This change in state is accompanied by a relatively large change in thermal entropy (85.6 $J\,mol^{-1}\,K^{-1}$) [16].

The spin-label partitioning probe serves as a reporter of the structural organization of the membrane and the perturbations induced by ethanol. The Tempo partitioning traces as a function of temperature are shown in Fig. 3. The partitioning traces are fit to the appropriate modification of Eqn. 1 for a three-state/two-equilibria system to yield partition coefficients for each state, the midpoint temperatures, and the sharpness of the interchange. All three membrane structures exhibit a characteristic receptivity to Tempo partitioning. In Fig. 3A, a jump in partitioning from 0.96 to 6.8 molal units at 33.9°C marks the transformation from the gel structure to the ripple structure. A jump in partitioning from 7.9 to 26.9 molal units at 41.2°C marks the transformation from a ripple structure to a liquid-crystalline fluid-bilayer structure.

Each succeeding panel in Fig. 3 represents a sequential increase in ethanol concentration. The low entropy, $L_{\beta'} \rightarrow P_{\beta'}$, interchange is perturbed and shifted to lower temperature by ethanol to a much greater extent than the relatively high entropy, $P_{\beta'} \rightarrow L_\alpha$, interchange. The essential point is that these equilibria exhibit different sensitivities to the action of ethanol. The membrane equilibrium that involves a low thermal entropy change is 5.3-times more sensitive to ethanol than the membrane equilibrium with a large thermal entropy change.

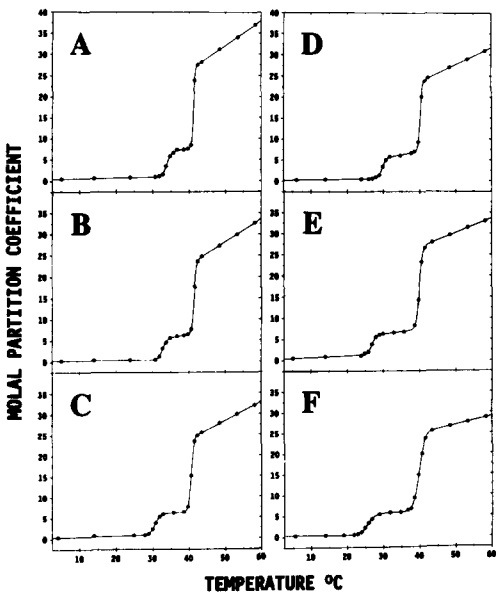

Fig. 3. The molal partition coefficients of Tempo in DPPC are shown as a function of temperature and ethanol concentration: (A) 0 mM ethanol; (B) 100 mM ethanol; (C) 300 mM ethanol; (D) 500 mM ethanol; (E) 750 mM ethanol; (F) 1 M ethanol. The lines represent a least-squares fit to the data according to Eqn. 1.

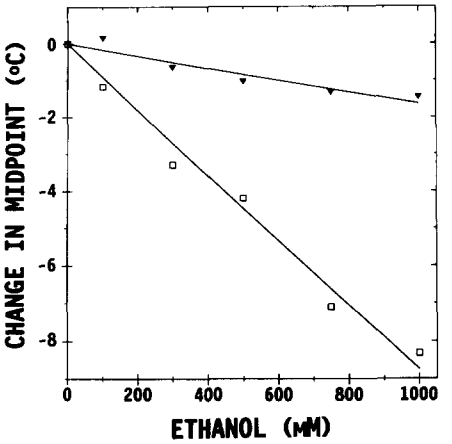

Fig. 4. The dependence of the midpoint temperature on the ethanol concentration. Triangles represent the $P_{\beta'} \rightarrow L_\alpha$ equilibrium, and squares represent the $L_{\beta'} \rightarrow P_{\beta'}$ equilibrium. The solid lines are fits according to Eqn. 5.

According to the generalized colligative thermodynamic treatment embodied in Eqn. 5, the action of ethanol is determined by the ratio of the configurational entropy imparted through the partitioning process and the thermal entropy characteristic of the equilibrium. The thermal entropy of the equilibrium is known from calorimetry, and is reported to be approximately constant for the solute levels employed here [28,29]. The ethanol-induced perturbation of the equilibrium midpoint temperature is determined by analysis of the Tempo partitioning curves in Fig. 3. Thus, the only remaining unknown in Eqn. 5 is the difference in configurational entropy between structures that is the driving force of the perturbation. The potency of ethanol in modulating the midpoint of the equilibrium is shown in Fig. 4. Fitting the data to Eqn. 5 yields the difference in configurational entropy between the two structures involved in the equilibrium and, consequently, the difference in the ethanol partitioning between those structures. The fit indicates that the difference in ethanol partitioning among membrane structures is constant over the range of ethanol examined. The partitioning difference between the gel and the ripple-structures is 0.062 molal units, whereas the partitioning difference between the ripple and the fluid bilayer-structure is 0.079 molal units.

Ethanol and cooperativity

The cooperativity of an equilibrium is a measure of the sharpness of the transition and reflects the size of the lipid assembly that undergoes a concerted conformational change. Since the conformation of a single lipid molecule is restricted by its neighbors, these membrane equilibria involve a collective conformational change of a lipid assembly. Many lipophilic agents are believed to decrease the cooperativity of membrane equilibria [30]. The full-width at half-height of the derivatives to the partitioning traces in Fig. 3 provides a measure of cooperativity [17] ($L_{\beta'} \rightarrow P_{\beta'}$: 0 mM, 2.1°C; 100 mM, 2.1°C; 300 mM, 2.5°C; 500 mM, 1.9°C; 750 mM, 1.9°C; $P_{\beta'} \rightarrow L_{\alpha}$: 0 mM, 0.73°C; 100 mM, 1.1°C; 300 mM, 1.3°C; 500 mM, 1.0°C; 750 mM, 1.57°C). We observe little or no loss of cooperativity induced by 750 mM ethanol in agreement with previous reports for the $P_{\beta'} \rightarrow L_{\alpha}$ equilibrium [21,30]. The scatter is within the uncertainty, ± 0.5°C, associated with the sampling rate of Tempo partitioning (one degree increments near the midpoints). At 1 M ethanol, however, the widths broaden to 3.6°C and 2.7°C, respectively, which may reflect the initial structural perturbations that lead to lipid interdigitation. The onset of these perturbations occur at 1.02 M and are reflected by an increase in the main transition temperature and ultimately a sharper, more cooperative transition [31,32].

Tempo partitioning

Tempo is an anesthetic spin-label that at low concentrations serves as a virtually nonperturbing partitioning probe that reports on the structural alterations of the membrane induced by ethanol. Other features of Tempo partitioning that are peripheral to its main function as a reporter of membrane structure are worth comment. Tempo partitioning exhibits an unusually large-positive temperature-dependence of partitioning, that is apparent in all three membrane structures, but most pronounced in the fluid bilayer structure. This positive temperature dependence is attenuated in the presence of ethanol (slope (L_{α}): 0 mM, 0.59; 100 mM, 0.54; 300 mM, 0.45; 500 mM, 0.41; 750 mM, 0.35; 1 M, 0.21). Since ethanol partitions much more strongly into water than into the membrane on a molal basis, and since the partition coefficient depends on the relative attractive forces of both the aqueous and membrane environments, it is uncertain whether the decreased temperature-dependence of Tempo partitioning induced by ethanol is due to membrane-bound ethanol, free aqueous ethanol or both.

The change in Tempo partitioning between states at the midpoint in Fig. 3 exhibits no obvious dependence on ethanol ($P_{\beta'} \rightarrow L_{\alpha}$: 18.1 ± 1.2 (S.D.) molal units; $L_{\beta'} \rightarrow P_{\beta'}$: 5.1 ± 0.4 (S.D.) molal units).

Discussion

Configurational entropy as the driving force of ethanol action

The main question this work addresses is the following. What membrane processes are sensitive to ethanol and what are the physical origins of the sensitivity? We have developed a generalized colligative thermodynamic framework that implicates configurational entropy as the driving force of ethanol action on cooperative equilibria in membranes. Configurational entropy is the positional randomness imparted by ethanol to the membrane in the partitioning (or mixing) process.

The hypothetical free energy diagrams in Fig. 5 encapsulate the essence of the energetic arguments for

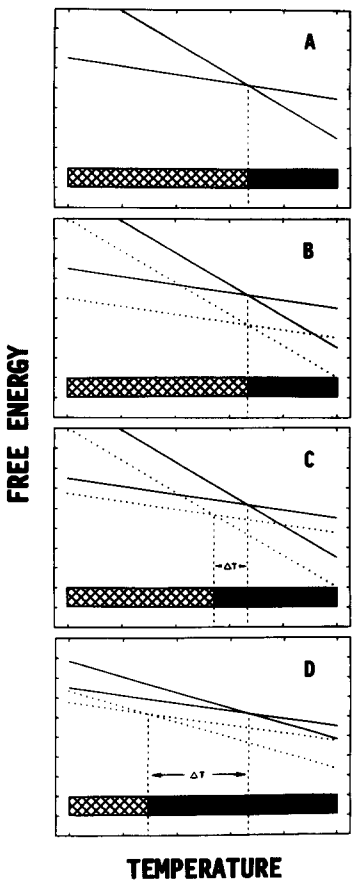

Fig. 5. Schematic and hypothetical free energy diagrams showing the action of ethanol on phase equilibria between two membrane structures. The free energy of two hypothetical structures in the absence of ethanol is represented by the solid lines. The dotted lines, lying below and parallel to the solid lines, represent the free energy lowering caused by ethanol. The crosshatched and shaded bars correspond to the two structures and represent the range of temperatures over which each structure exists in the presence of ethanol. (A) The equilibria unmodified by ethanol. (B) As in (A), but in the presence of ethanol for the case where ethanol partitions equally into both structures. (C) As in (B), except that ethanol partitioning is reduced two-fold in the low temperature structure. (D) As in (C) except that the molar entropies of the structures (slopes of the lines) are more equal.

ethanol action through configurational entropy. The free energy of a state (G) is defined

$$G = -S \cdot T + H \quad (6)$$

For purposes of clarity, both the enthalpy (H) and entropy (S) are assumed constant (independent of temperature; therefore, the weak curvature expected for the lines is neglected). In panel 5A, the free energies of two hypothetical structures as a function of temperature are represented by the solid lines. The intersection of the lines is the equilibrium midpoint temperature, at which point the free energies are equal, ΔG is zero, and K_{eq} is one. Above or below the midpoint temperature the structure with the lowest free energy is thermodynamically favored, represented by the crosshatched and shaded bars.

Panel 5B demonstrates the effect of ethanol. Shown is the hypothetical situation for ethanol partitioning equally into each structure of the equilibrium. The configurational entropy imparted by the dissolution of ethanol into the membrane lowers the free energy of the membrane structure, represented by the parallel dotted lines. The dotted lines exhibit a slightly increased slope that is ignored for the sake of simplicity. Since the partitioning into each state in Panel B is equal, the lowering of the free energy is equal, and there is no change in the relative free energies or equilibrium midpoint. Therefore, a prerequisite for ethanol action via configurational entropy are partitioning differences between membrane structures. Conversely, agents that partition uniformly will induce no net effect, consistent with lipophiles that lack anesthetic potency. This observation distinguishes this model for ethanol action from the Gibbs free energy hypothesis proposed by Hill [19,20].

Panel 5C illustrates the basis whereby partitioning differences among structures modulates the equilibrium between those structures. The diagram is unchanged from Panel 5B except that the partitioning into the low-temperature structure is decreased by half. Since the partitioning of ethanol into the high-temperature structure is greater and the free energy lowering is greater, this structure is stabilized at the expense of the low-temperature structure and exists over a wider temperature range. If, instead, partitioning was greater into the low temperature structure the midpoint would have been raised, not lowered (thus raising the possibility that some agents may antagonize anesthesia).

Panel 5D illustrates the basis for our postulate that equilibria that involve small changes in entropy are more susceptible to the action of ethanol. The slopes of the free energy traces are determined by entropy (Eqn. 6). If the slopes are similar, then the entropies of each structure are similar, and the entropy change of the equilibrium is similar. In panel 5D, the slope of the high-temperature state is reduced so that the entropies of both states are similar. Although the partitioning is unchanged from panel 5C, the effects of partitioning are much greater and a dramatic shift in the midpoint temperature is observed.

Panels 5C and 5D exemplify the energetics that underlie ethanol action in the lecithin membrane examined here, and the generalized principles for the action of all lipophilic solutes expressed in Eqn. 5. The difference in thermal entropy between the ripple and fluid bilayer states is large, so that the configurational entropy imparted by ethanol induces a modest perturbation similar to the free energy diagram shown in 5C. Conversely, the gel and ripple states exhibit similar thermal entropies, so that the configurational entropy imparted by ethanol induces a more substantial perturbation as shown in 5D.

Fig. 5 also illustrates the basis for the equivalence of the action of ethanol with the action of temperature. Both act through entropy to alter the energetic balance among membrane structures. Arguments against lipid theories of ethanol action center on the observation that pharmacological concentrations of ethanol induce membrane perturbations that are commensurate with perturbations that accompany normal variations in body temperature. Colligative thermodynamics supports the validity of such temperature/ethanol comparisons of effects on membrane architecture, and suggests that insensitivity is not an inherent feature of alcohol–membrane interactions.

Changes in membrane-lipid order-parameters (fluidity) may also play an important role in determining ethanol action [2,7,8]. Fluidization induced by ethanol, however, is modest in temperature equivalents [10]. In the thermodynamic framework, changes in membrane order are considered an important colligative reflection of the underlying physical processes, but not the mode of action per se.

Partition coefficients of ethanol

As a weak anesthetic, ethanol exhibits a weak lipophilicity and membrane partitioning. The determination of such small partition coefficients poses experimental difficulties; consequently, the partitioning behavior of ethanol into membranes is more controversial than the partitioning behavior of more lipophilic, longer chain alcohols. In this study, we have reported the ability of ethanol to modulate the midpoint temperatures of two equilibria and used a colligative thermodynamic model that relies on reported calorimetric thermal entropy changes to report differences in partitioning between membrane structures. On this basis, we conclude that partitioning into the ripple structure is 0.062 molal units greater than the gel structure, and that partitioning into the fluid bilayer structure is 0.079

molal units greater than the ripple structure. Total partitioning into the fluid bilayer structure is the sum, 0.14, plus a small contribution anticipated from gel-structure partitioning and a contribution anticipated from slight, probably positive, temperature-dependence of partitioning in each structure [5].

Previously, we have validated the thermodynamic approach with direct lecithin binding studies for hexanol and benzyl alcohol [13–15]. The membrane perturbations induced by these alcohols were quantitatively reproduced by the predictions of the colligative thermodynamic model using directly measured partitioning. The molal partition coefficients for benzyl alcohol in DPPC are 0.88 in the gel-structure, 5.24 in the ripple-structure, and 13.2 in the fluid bilayer-structure [15]. The molal partitioning of dilute n-hexanol in the related lecithin, DMPC (1,2-dimyristoyl-*sn*-glycero-3-phosphocholine), was 1.3, 23.5, 91.7, respectively [13]. The relative partitioning changes deduced for ethanol in this work are qualitatively similar to these longer chain alcohols. A large ethanol partitioning change coincides with the interchange between the ripple to fluid bilayer-structures (0.079), and a substantial, though somewhat smaller change, coincides with the interchange between the gel and ripple-structures (0.062).

A simplified colligative thermodynamic treatment of alcohol action was first implemented by Hill using a freezing point depression model to relate changes in the main transition midpoint temperature to partitioning [19,20]. That model considered partitioning into the fluid-bilayer structure only. In the generalized colligative framework developed here, the partition coefficients obtained using Hill's approach are not absolute measures of partitioning, but are *differences* in partitioning between the ripple and fluid-bilayer structures at the midpoint. Reported molal partitioning differences between the ripple and the fluid-bilayer structure using Hill's approach are 0.046 [22], 0.078 [20] and 0.112 [21]. All values have been recalculated from the original using the more recently reported thermal entropy change employed here and are directly comparable to our value for this partitioning difference, 0.079. These values correspond to potencies ranging from −0.11 to −0.25°C per 100 mM ethanol (this work, −0.17°C). This two-fold variation in potencies reported by different laboratories reflects an insensitivity to solutes that is expected for large thermal entropy changes; consequently, the resulting perturbations rival experimental uncertainties in temperature.

Implications for biological membranes

The lecithin structures examined here were chosen because their properties are well-established and because the equilibria are characterized by substantially different molar thermal entropies. This provides a test of the thermodynamic prediction that the ethanol-induced perturbations arise from competing contributions of entropy. The model equilibria do not 'solve' the insensitivity issue for lipid theories of anesthesia. General anesthetic concentrations of ethanol range from about 100–300 mM, which corresponds to a modest perturbation of the low entropy equilibrium. The model provides a simple validation for the thermodynamic framework and its premise that insensitivity to anesthetics is not an inherent feature of lipid organization in membranes. No putative biological relevance for either equilibrium in eukaryotes per se should be inferred. Rather, it is the energetic features that distinguish the low entropy interchange from the high entropy interchange that are postulated to be common to ethanol-sensitive equilibria in biological membranes, and may be characteristic of the locus for anesthesia.

Biological membranes are increasingly understood as a structurally diverse and heterogeneous two-dimensional fluid composed of a dynamic mosaic of microdomains which are energetically balanced for sensitivity to chemical stimulus. All processes that are dependent on a defined membrane architecture are susceptible to disturbance by alcohol and anesthetics. Proteins that require defined lipid domains are potential targets, as are membrane trafficking and fusion events. Domain structure may dictate lateral compartmentation that determines protein-protein and protein-ligand accessibility. In the partitioning process, ethanol stabilizes each domain depending on the degree of partitioning. When partitioning is unequal among domain structures, ethanol acts to alter the free energy change, and the equilibrium balance among domains. Assessed from the vantage of the *average* free energy of the membrane, the action of ethanol is equivalent to a mosaic of local thermal heating and cooling that alters the energetic balance that maintains native membrane architecture.

Acknowledgements

This work was supported by US Public Health Service Grants AA07186, AA00088, AA07215, and AA07463.

References

1 Hunt, W.A. (1985) Alcohol and Biological Membranes, Guilford Press, New York.
2 Taraschi, T.F. and Rubin, E. (1985) Lab. Invest. 52, 120–131.
3 Meyer, H. (1899) Arch. Exp. Pathol. Pharmakol. (Naunyn-Schmiedeberg) 42, 109–118.
4 Overton, C.E. (1991) Studies of Narcosis Chapman and Hall, New York.
5 Janoff, A.S. and Miller, K.W. (1982) in Biological Membranes (Chapman, D., ed.), Vol. 4, pp. 417–476, Academic Press, New York.

6 Hill, M.W. and Bangham, A.D. (1975) Adv. Exp. Med. Biol. 59, 1–9.
7 Chin, J.H. and Goldstein, D.B. (1977) Science 196, 684–685.
8 Rottenberg, H., Waring, A. and Rubin, E. (1981) Science 213, 583–585.
9 Hoek, J.B., Taraschi, T.F. and Rubin, E. (1988) Semin. Liver Disease 8, 36–46.
10 Franks, N.P. and Lieb, W.R. (1987) Alcohol Alcoholism Suppl.1, 139–145.
11 Franks, N.P. and Lieb, W.R. (1984) Nature 310, 599–601.
12 Moss, G.W.J., Lieb, W.R. and Franks, N.P. (1991) Biophys. J. 60, 1309–1314.
13 Janes, N., Hsu, J.W., Rubin, E. and Taraschi, T.F. (1992) Biochemistry 31, 9467–9472.
14 Janes, N., Hsu, J.W., Rubin, E. and Taraschi, T.F. (1991) Biophys. J. 59, 125a.
15 Ma, L., Taraschi, T.F., and Janes, N. (1992) Bull. Magn. Reson., in press.
16 Chen, S.C. and Sturtevant, J.M. (1981) Biochemistry 20, 713–718.
17 McElhaney, R.N. (1982) Chem. Phys. Lipids 30, 229–259.
18 Bent, H.A. (1965) The Second Law, Oxford University Press, New York.
19 Hill, M.W. (1974) Biochim. Biophys. Acta 356, 117–124.
20 Hill, M.W. (1975) Biochem. Soc. Trans 3, 149–152.
21 Rowe, E.S. (1982) Mol. Pharmacol. 22, 133–139.
22 Kamaya, H., Kaneshina, S. and Ueda, I. (1981) Biochim. Biophys. Acta 646, 135–142.
23 Kaminoh, Y., Tashiro, C., Kamaya, H. and Ueda, I. (1988) Biochim. Biophys. Acta 946, 215–220.
24 Suezaki, Y., Tatara, T., Kaminoh, Y., Kamaya, H. and Ueda, I. (1990) Biochim. Biophys. Acta 1029, 143–148.
25 Kaminoh, Y., Nishimura, S., Kamaya, H. and Ueda, I. (1992) Biochim. Biophys. Acta 1106, 335–343.
26 McConnell, H.M., Wright, K.L. and McFarland, B.G. (1972) Biochem. Biophys. Res. Commun. 47, 273–281.
27 Schreier, S., Polnaszek, C.F. and Smith, I.C.P. (1978) Biochim. Biophys. Acta 515, 395–436.
28 Mountcastle, D.B., Biltonen, R.L. and Halsey, M.J. (1978) Proc. Natl. Acad. Sci. USA 75, 4906–4910.
29 Sturtevant, J.M. (1982) Proc. Natl. Acad. Sci. USA 79, 3963–3967.
30 Jain, M.K. and Wu, N.M. (1977) J. Membr. Biol. 34, 157–201.
31 Simon, S.A. and McIntosh, T.J. (1984) Biochim. Biophys. Acta 773, 169–172.
32 Rowe, E.S. (1985) Biochim. Biophys. Acta 813, 321–330.